Hindawi Publishing Corporation
Mathematical Problems in Engineering
Volume 2016, Article ID 9596089, 11 pages
http://dx.doi.org/10.1155/2016/9596089

Research Article

Multidisciplinary Design Optimization of Crankshaft Structure Based on Cooptimization and Multi-Island Genetic Algorithm

Jian Liu, Gaoyuan Yu, Yao Li, Hongmin Wang, and Wensheng Xiao

Research Center for Marine Oil-Gas Equipment and Security Technology, China University of Petroleum (East China), Qingdao 266580, China

Correspondence should be addressed to Gaoyuan Yu; 961023731@qq.com

Received 11 November 2015; Accepted 19 May 2016

Academic Editor: Burak Eksioglu

The feasibility design method with multidisciplinary and multiobjective optimization is applied in the research of lightweight design and NVH performances of crankshaft in high-power marine reciprocating compressor. Opt-LHD is explored to obtain the experimental scheme and perform data sampling. The elliptical basis function neural network (EBFNN) model considering modal frequency, static strength, torsional vibration angular displacement, and lightweight design of crankshaft is built. Deterministic optimization and reliability optimization for lightweight design of crankshaft are operated separately. Multi-island genetic algorithm (MIGA) combined with multidisciplinary cooptimization method is used to carry out the multiobjective optimization of crankshaft structure. Pareto optimal set is obtained. Optimization results demonstrate that the reliability optimization which considers the uncertainties of production process can ensure product stability compared with deterministic optimization. The coupling and decoupling of structure mechanical properties, NVH, and lightweight design are considered during the multiobjective optimization of crankshaft structure. Designers can choose the optimization results according to their demands, which means the production development cycle and the costs can be significantly reduced.

1. Introduction

New marine reciprocating compressors must have high power, high pressure ratio, and slight vibration and be environmentally friendly with the development of marine natural gas boosting and gathering [1]. Therefore, the effect of each component of the compressors on its overall performance should be investigated in detail. Crankshaft systems of reciprocating compressors have an effective influence on compressor performance, being the main part responsible for vibration production [2].

The high-power reciprocating compressors are designed to run onshore; accordingly, the support of compressors cannot match the crankshaft structure parameters and there are some drawbacks such as loud noise and high vibration intensity caused by gas force, reciprocating inertia force, and centrifugal force when it is used offshore [3–5]. Consequently, the parameters of crankshaft structure should be changed. To study parameters effect will face longer time period, higher experimental cost, and complicated verification process through the experiment of compressor [6].

The crankshaft structure is a complex engineering system involving structural mechanics, mechanical vibration and noise, and man-machine-environment engineering. The crankshaft structure design is a complex multidisciplinary and multistage design process relating to high correlation and coupling between all disciplines. The whole process can be described by a complex function. The optimized parameters combination of crankshaft structure is obtained by iterating and optimizing. Consequently, it is a key factor to choose a suitable algorithm to solve this issue. Studies on crankshaft of reciprocating compressors mainly focus on vibration and stress analyses [7–10]. Although stress analyses of crankshafts are available in literature, there are few studies on the optimization of crankshaft. Almasi [6] optimized the configuration of the compressor critical components to improve the performance and reliability. Yang et al. [11] introduced a new approach to analyses vibration performance of small reciprocating compressor on the basis of artificial neural networks and support vector machines. And the classification of compressor is achieved. Benini [12] proposed

a multiobjective optimization algorithm in transonic compressor rotor structure and improved the pressure ratio. Ho et al. [13] improved the crankshaft reliability by Monte Carlo simulation on the basis of the finite element model. Although the algorithms mentioned earlier are effective in obtaining the optimal solution, comprehensive design is difficult to achieve by single discipline. Therefore, multidisciplinary design optimization (MDO) theory is necessary to achieve the comprehensive design of crankshaft [14, 15].

Although multiple parameters affect the performance of compressor, the amount of data obtained by compressor experiment is limited. The EBFNN theory is good at solving small sample learning problems [16, 17]. Due to its strong ability of nonlinear function approximation and excellent generalization capacity, EBFNN has been widely used in the field of industrial engineering.

In this paper, the coupling and interdisciplinary relationships of mechanical properties, NVH, and lightweight are considered and the MDO technology roadmap of the reciprocating compressor was proposed on the basis of virtual proving ground (VPG) technology. Cooptimization based on EBFNN and multi-island genetic algorithm is applied to the multiobjective optimization of crankshaft structure in order to gain the Pareto optimal solution set.

2. MDO of the Crankshaft Structure

The MDO theory is applied in crankshaft structure design on the basis of VPG. The flow chart of the enforceable technology roadmap is shown in Figure 1.

The crankshaft MDO issues mainly focus on the effective optimization strategy to achieve concurrent design of multidisciplinary subsystems and obtain the satisfactory solution. The strategy combines the knowledge from different subjects with optimization algorithm and develops an effective method to solve the complex problems [18, 19].

The MDO optimization framework can be divided into single-stage and multiple-stage. The single-stage optimization framework is composed of multidisciplinary feasible method (MDF) and individual discipline feasible method (IDF). The multistage optimization framework consists of concurrent subspace optimization (CSSO), cooptimization (CO), and bilevel integrated (Bliss).

In this paper, the CO is mainly studied. CO is a multistage MDO algorithm on the basis of the optimization algorithm under consistency constraints. It divides the crankshaft MDO issues into one system-level optimization and multiple subsystem-level optimization.

The system-level optimization objective of crankshaft can be expressed as

$$\begin{aligned} &\min \quad F(Z) \\ &\text{s.t.} \quad J_i(Z) < \varepsilon \quad i = 1, 2, \ldots, n. \end{aligned} \tag{1}$$

The subsystem-level optimization objective of crankshaft is listed as

$$\min \quad J_i(Z) = \left|X_i - Z_i\right|^2 + \left|Y_i - Z_i\right|^2$$

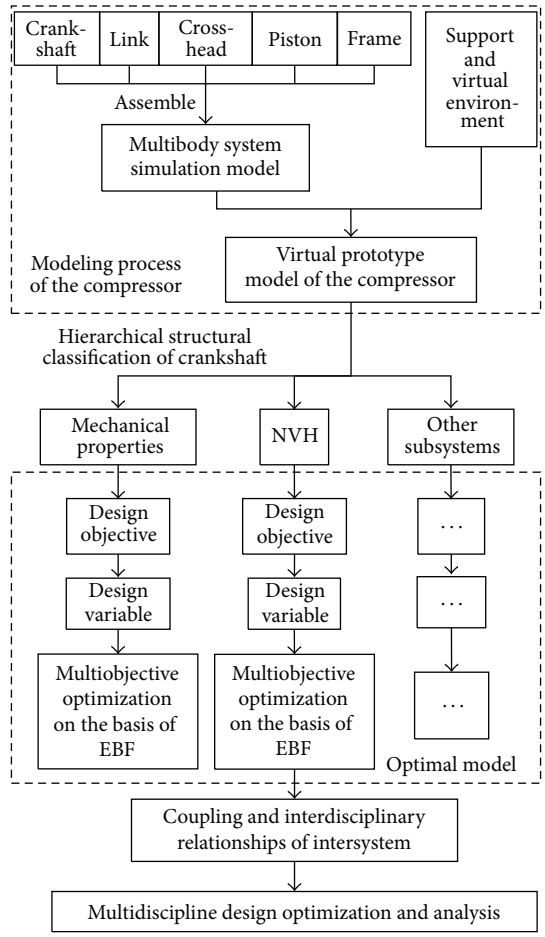

Figure 1: MDO technology roadmap on the basis of VPG.

$$\begin{aligned} \text{s.t.} \quad & G_u(Z) < 0 \quad u = 1, 2, \ldots, p \\ & H_v(Z) = 0 \quad v = 1, 2, \ldots, q. \end{aligned} \tag{2}$$

The meaning of the symbols in the formula is shown as follows:

X_i: design variable of i subsystem.

Y_i: state variable of i subsystem.

Z_i: target expectation of system-level design variable.

F: system-level objective function.

$J_i(Z)$: objective function of i subsystem.

$G_u(Z)$: inequality constraint of i subsystem.

$H_v(Z)$: equality constraint of i subsystem.

p: quantity of the corresponding function.

q: quantity of the corresponding function.

ε: slack variable.

3. Multiobjective Optimization Problems and Solving

3.1. Multiobjective Optimization Problem. Multiobjective optimization problem (MOP) of crankshaft can be represented as

$$\begin{aligned} \min \quad & y = F(x) = \left(f_1(x), f_2(x), \ldots, f_n(x)\right) \\ \text{s.t.} \quad & g_i(x) < 0 \quad i = 1, 2, \ldots, l \\ & h_j(x) = 0 \quad j = 1, 2, \ldots, m \\ & x_L \le x \le x_U \quad x = \left(x_1, x_2, \ldots, x_r\right) \in X. \end{aligned} \tag{3}$$

The meaning of the symbols in the formula is shown as follows:

y: target vector, which can represent the optimization objectives of mechanical properties, NVH, and other subsystems of the crankshaft.

$g_i(x)$: equality constraint of i subsystem.

$h_j(x)$: equality constraint of i subsystem.

x: decision vector.

x_L: lower bound of decision vector.

x_U: upper bound of decision vector.

X: decision space formed by decision vector.

l: quantity of the corresponding function.

m: quantity of the corresponding function.

n: quantity of the corresponding function.

r: quantity of the corresponding function.

With the given crankshaft MOP issue, the Pareto optimal solution can be defined as follows: if and only if there exists no feasible solution (x_B belongs to X) which makes $F(x_B)$ better than $F(x_A)$, will x_A belongs to X be one of the Pareto optimal solutions. Hence, the optimal Pareto set can be represented as

$$x_f = \left\{x_A \in X \mid \forall x_B \notin X \mid F\left(x_B\right) > F\left(x_A\right)\right\}. \tag{4}$$

Inevitably, the MDO of the crankshaft is accompanied by the MOP of the crankshaft. MOP of the crankshaft cannot achieve best possible optimization of all objectives simultaneously and arbitrary solution of Pareto set will possibly become the satisfactory solution.

3.2. Solving of MOP. The evaluation methods of MOP can be divided into global optimization algorithms and local optimization algorithms. The global optimization algorithms include genetic algorithm, simulated annealing algorithm, particle swarm optimization, and ant colony algorithm. Due to their high capability of global search, high speeds of convergence, and search results independent on starting point, the global optimization algorithms are capable of solving high dimensional and nonlinear problems. But the computation might be expensive and sometimes unsatisfactory local optimization effect [20–22]. The local optimization algorithms include constraint algorithm, weighting algorithm, distance function algorithm, and gradient descent algorithm. The local optimal optimization algorithms mentioned earlier have a strong ability in finding the local optimal solution, but it is difficult to choose the starting point of high dimensional and nonlinear problems [23, 24]. Hence, multi-island genetic algorithm is chosen to solve the application issue. The multi-island algorithm can maintain optimal solution diversity and improve the local optimization effect by interisland migration on the basis of traditional genetic algorithm [25]. The flow chart of MIGA is shown in Figure 2.

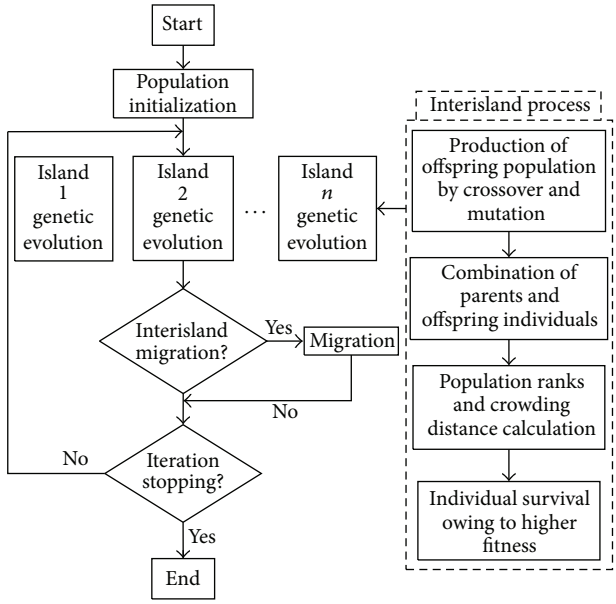

Figure 2: Flow chart of MIGA.

4. Multiobjective Optimization of Crankshaft

4.1. NVH Simulation of Crankshaft. The modal analysis is an important part of dynamic analysis in reciprocating compressor machine system, which can help us understand the dynamic characteristic of the system. The natural frequency of crankshaft is usually calculated to avoid resonances during use in the design of NVH. Severe deforming parts of crankshaft are observed to judge the strength of the corresponding structure, which may become noise vibration source or main transfer path and should be modified early.

There are 269612 entity units and 452154 nodes on the finite element model of crankshaft NVH. The characteristic of NVH is studied by crankshaft modal analysis and torsional vibration.

The crankshaft modal is computed by ANSYS under free boundary. Therefore, the first-order natural frequency is 41.413 Hz. The second-order natural frequency is 43.54 Hz.

In the process of the torsional vibration analysis, the modal superposition method is used to simplify the finite element of crankshaft. The elastic deformation of the structure is solved approximately by linear combination of suitable modes which can be shown as follows:

$$[u] = [\varphi][q]. \tag{5}$$

The meaning of the symbols in the formula is shown as follows:

$[u]$: displacement matrix.

$[\varphi]$: modal shape function matrix.

$[q]$: vector of modal coordinates.

An elastic body contains two types of nodes, interface nodes, where forces and boundary conditions interact with the structure during multibody system simulation (MSS), and interior nodes. In MSS the position of the elastic body is computed by superposing its rigid body motion and elastic deformation. In ADAMS, this is performed using "Component Mode Synthesis" technique based on Craig-Bampton method [8, 9]. The component modes contain static and dynamic behavior of the structure. The modal transformation between the physical DOF and the Craig-Bampton modes and their modal coordinates is described by [2]

$$[u] = \begin{Bmatrix} u_B \\ u_1 \end{Bmatrix} = \begin{bmatrix} I & 0 \\ \varphi_C & \varphi_N \end{bmatrix} \begin{Bmatrix} q_C \\ q_N \end{Bmatrix}. \quad (6)$$

The meaning of the symbols in the formula is shown as follows:

u_B: column vectors of boundary DOF.

u_1: column vectors of interior DOF.

I: identity matrix.

0: zero matrix.

φ_C: matrix of physical displacements of the interior DOF in the constraint modes.

φ_N: matrix of physical displacements of the interior DOF in the normal modes.

q_C: column vector of modal coordinates of the constraint modes.

q_N: column vector of modal coordinates of the fixed boundary normal modes.

To obtain decoupled set of modes, constrained modes and normal modes are orthogonalized.

The crankshaft system model is shown in Figure 3. Elastic 3D solid crankshaft model of reciprocating compressor is obtained in ANSYS using modal superposition method. First, 3D solid model of the crankshaft is imported to ANSYS and finite element model of the crankshaft is obtained. Flexible crankshaft model is obtained through modal synthesis considering the first 30 fixed boundary normal modes. Then, this model is imported to ADAMS/View and 3D finite element model is run with ADAMS.

4.2. Strength of Crankshaft. The boundary condition of crankshaft strength analysis is shown in Figure 4. The radial and axial freedom of main bearings from ① to ⑥ are constrained. Forces in a reciprocating compressor can be divided into gas forces, piston lateral impact forces, and inertia forces. The gas forces are applied on the prismatic pairs of piston. Then, excitation force and torque acted on the crankpin from I to VI are obtained by MSS. In the calculation example, the rotate speed of crankshaft is set to 994 r/min, the manifold pressure is set to 2.0 Mpa, and the exhaust pressure is set to 6.0 Mpa. The type of cylinder is double-acting.

Figure 3: Model of crankshaft system.

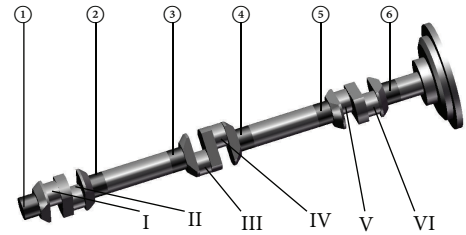

Figure 4: Boundary condition of crankshaft strength analysis.

5. Multidisciplinary Optimization of Crankshaft

The deterministic optimization, reliability optimization, and multiobjective optimization are operated independently on the basis of EBFNN and CO. The flow chart of MDO is shown in Figure 5.

5.1. System Decomposition. Systems in crankshaft structure can be divided into mass, NVH, and strength subsystem. The NVH subsystem includes modal analysis and torsional vibration.

5.2. Design Variable. The structure of crankshaft system has an important effect on the torsional vibration, strength, natural frequency, and mass of crankshaft. As the crankshaft is constrained by the dimension and assembly of connecting rod, frame, and other parts, the dimension of crank journals, crankpins, and bore spacing cannot be changed in this calculation example. Consequently, transitional fillet (x_1), oil passage (x_2), and shape parameters of lightening holes (x_3, x_4, x_5) are chosen as the design variables, which is shown in Figure 6.

5.3. Experiment Design. Opt-LHD is adopted to obtain the experimental scheme and perform data sampling. The elliptical basis function neural network (EBFNN) model considering modal frequency, static strength, torsional vibration

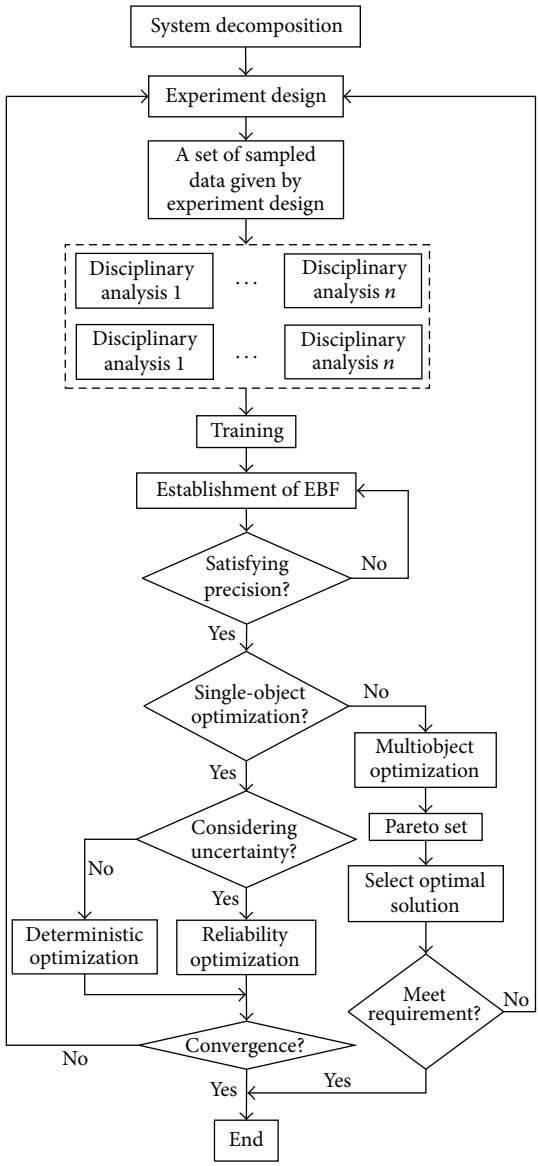

Figure 5: Flow chart of crankshaft system MDO.

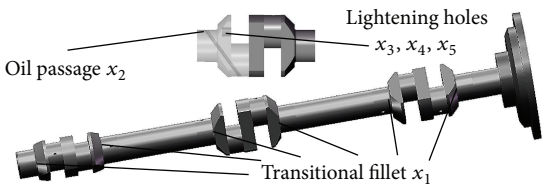

Figure 6: Design variables of MDO.

angular displacement, and lightweight design of crankshaft is built. The experimental scheme is listed in Table 1.

Targets in NVH subsystem include first-order modal frequency (f_1), second-order modal frequency (f_2), and the maximum torsional angular vibration over a period time ($\theta_{\max}$). Targets in strength subsystem include the maximum load on the main bearing over a period ($F_1, F_2, F_3, F_4, F_5, F_6$)

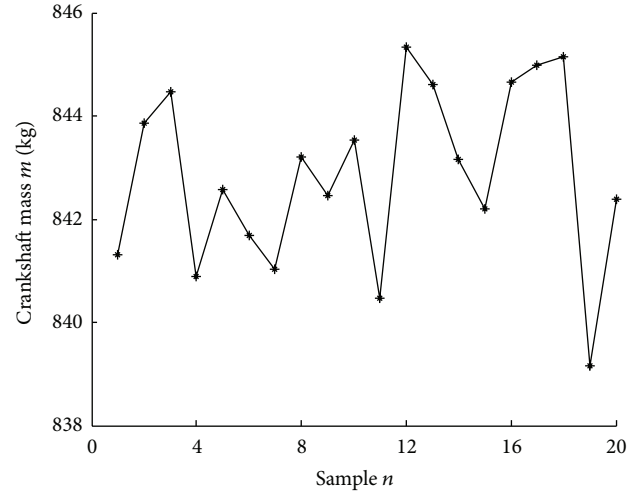

Figure 7: Result of crankshaft mass.

Table 1: Experimental scheme based on Opt-LHD.

Sample	Design variables				
	x_1	x_2	x_3	x_4	x_5
	mm	mm	mm	mm	mm
1	9.18	16.53	46.84	38.42	75.0
2	7.82	14.63	40.53	35.26	72.89
3	7.61	16.74	31.05	40.53	65.53
4	7.71	17.58	45.79	39.47	70.79
5	8.87	14.84	42.63	41.58	55.0
6	8.34	15.68	50.0	33.16	63.42
7	7.5	15.47	44.74	45.79	60.26
8	8.97	18.0	34.21	43.68	68.68
9	9.39	17.37	43.68	34.21	61.32
10	8.45	16.32	33.16	50.0	57.11
11	8.66	14.21	48.95	44.74	69.74
12	9.08	16.11	30.0	36.32	59.24
13	8.55	16.95	35.26	30.0	71.84
14	9.5	15.26	37.37	46.84	66.58
15	8.03	17.79	41.58	37.37	56.05
16	9.29	14.42	39.47	32.11	67.63
17	7.92	15.05	36.32	31.05	58.16
18	8.24	14.0	32.11	42.63	64.47
19	8.76	17.16	47.89	47.89	62.37
20	8.13	15.89	38.42	48.95	73.95

and the maximum stress over a period time ($\sigma_{\max}$). Mass of the crankshaft (m) is the target of the mass subsystem.

The time of training is set to 20 based on the parallel computing. The result is listed from Figures 7–11.

5.4. Surrogate Model. Each response is mapped to elliptical basis function surrogate model on the theory of the elliptical basis function neural network. It is shown in Figure 12.

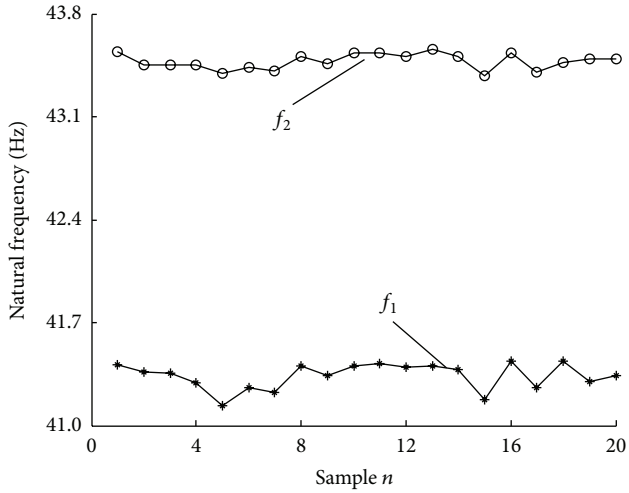

Figure 8: Result of modal frequency.

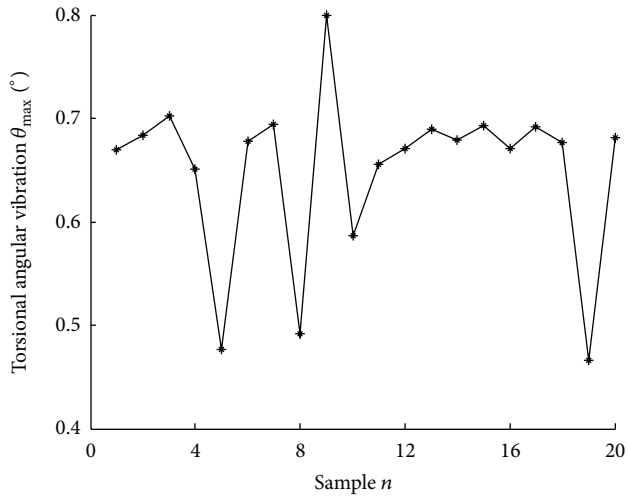

Figure 9: Result of the maximum of torsional angular vibration over a period time.

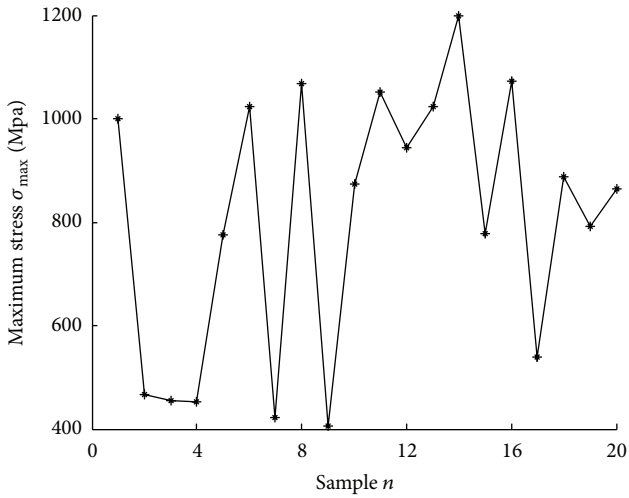

Figure 10: Result of the maximum stress over a period time.

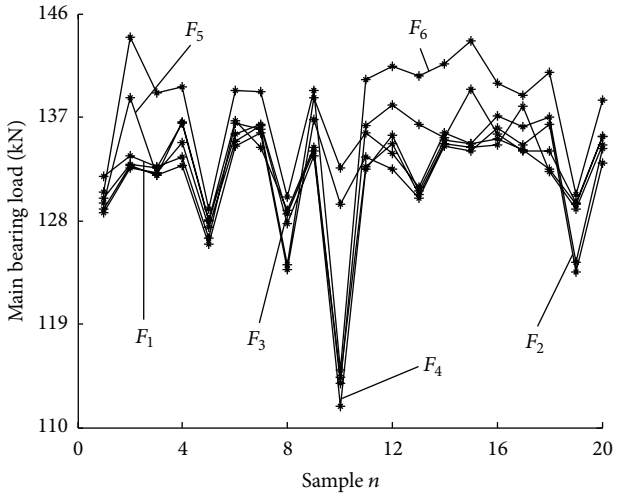

Figure 11: Result of main bearing load over a period time.

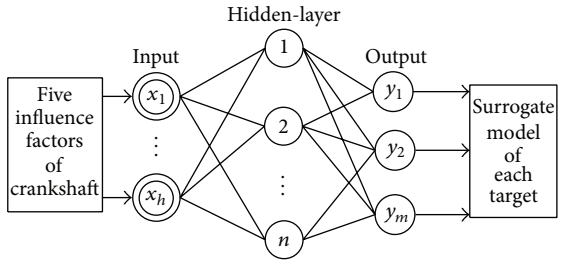

Figure 12: EBFNN model of crankshaft.

The elliptical basis function neural network including h input parameters, n hidden-layer nodes, and m output parameters can be described by

$$y_m(X) = \sum_{i=1}^{n} \left[\alpha_{mi} v_i(x)\right] + \alpha_{m(n+1)}. \quad (7)$$

The meaning of the symbols in the formula is shown as follows:

x: design variable.

α_{mi}: link weight between ith hidden-layer node and mth output parameter.

$v_i(x)$: base function by using Mahalanobis distance, which can be described by

$$v_i(x) = (x - x_i)^T S^{-1} (x - x_i). \quad (8)$$

The meaning of the symbols in the formula is shown as follows:

S: covariance matrix, which can be described by

$$S = \frac{1}{n} \sum_{i=1}^{n} (x_i - \mu)(x_i - \mu)^T. \quad (9)$$

Here, μ is the sample data center.

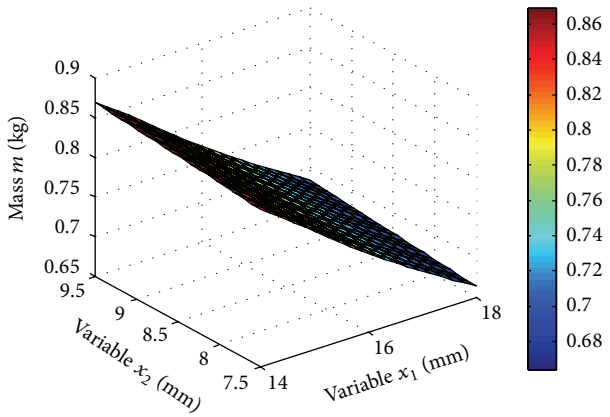

Figure 13: Response surface of mass normalization.

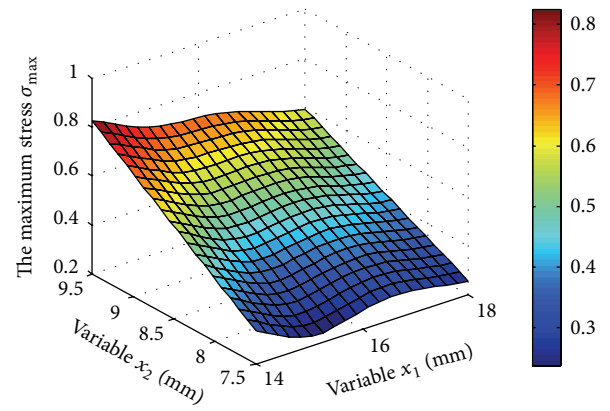

Figure 14: Response surface of the maximum stress normalization.

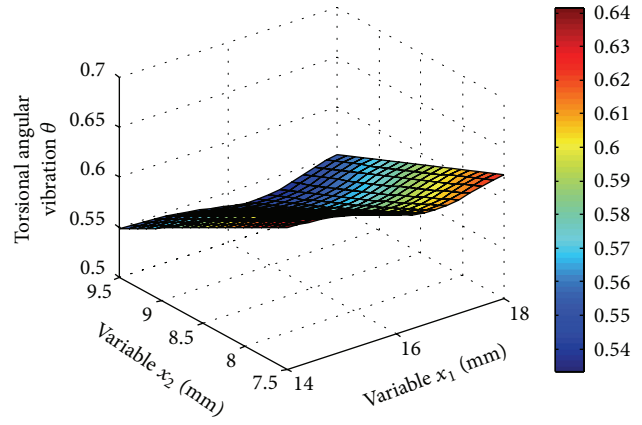

Figure 15: Response surface of torsional angular vibration normalization.

Having gained output responses $y = (y^{(1)}, y^{(1)}, \ldots, y^{(n)}, 0)$ corresponding to n samples, the connection matrix can be described by the following.

$$\alpha = \begin{bmatrix} \begin{bmatrix} v_1(x_1) & \cdots & v_1(x_n) \\ \vdots & \ddots & \vdots \\ v_n(x_1) & \cdots & v_n(x_n) \end{bmatrix} & \begin{matrix} 1 \\ \vdots \end{matrix} \\ \begin{matrix} 1 & \cdots \end{matrix} & 0 \end{bmatrix} y. \tag{10}$$

The tan-sigmoid function is used in this neural network. Hence, ideal output results should be close or equal to 1. The normalization processing of experiment data is carried out, which can be described by

$$Y_i = 0.1 + 0.8 \times \frac{y_i - y_{i\min}}{y_{i\max} - y_{i\min}}. \tag{11}$$

The meaning of the symbols in the formula is shown as follows:

Y_i: output values of normalization neural network.

y_i: experimental data.

$y_{i\min}$: the minimum experimental data.

$y_{i\max}$: the maximum experimental data.

The elliptical basis function surrogate model between design variables and its analysis target can be solved, combining formulas (6) to (11). The response surface of mass, torsional angular vibration, and the maximum stress are plotted in Figures 13–15.

As the elliptical basis function surrogate model between input variables and its analysis targets cannot be described by a specific function, correlation coefficients (R^2) are used to evaluate the degree of approximation between each model. The better the fitting of the surrogate model is, the closer the R^2 is to 1. The correlation coefficients can be described by

$$R^2 = 1 - \frac{\sum_{i=1}^{n} (y_i - Y)^2}{\sum_{i=1}^{n} (y_i - \overline{y})^2}. \tag{12}$$

The meaning of the symbols in the formula is shown as follows:

$\overline{y}$: average of sample response.

n: experiments.

The fitting of the surrogate model can be solved by formula (11) and formula (12). The correlation coefficient values of the elliptical basis function surrogate model corresponding to crankshaft mass, torsional angular vibration, and the maximum stress over a period time are more than 0.90. The results show that the surrogate model of the elliptical function can truly reflect function mapping between design variable and analysis objective. The approximate model corresponding to design variable is precise and can be used for optimization.

5.5. Single-Object Lightweight Optimization of Crankshaft. The deterministic system-level optimization objective can be represented as

$$\begin{aligned} &\min \quad M \\ &\text{s.t.} \quad J_i(Z) < \varepsilon \quad i = 1, 2, \ldots, n. \end{aligned} \tag{13}$$

The deterministic subsystem-level optimization objective can be represented as

$$\begin{aligned} \min \quad & J_i(Z) = \left|X_i - Z_i\right|^2 \\ \text{s.t.} \quad & \sigma_{\max} < [\sigma] \\ & \theta_{\max} \le [\theta] \\ & F_i \le F_{i0} \quad i = 1, 2, \ldots, 6 \\ & X_{j\mathrm{L}} \le X_j \le X_{j\mathrm{U}} \quad j = 1, 2, \ldots, 5. \end{aligned} \tag{14}$$

The meaning of the symbols in the formula is shown as follows:

ε: 10^{-5}.

$[\theta]$: allowable torsional angular vibration.

$[\sigma]$: allowable stress.

X_j: design variable of crankshaft, $j = 1, 2, 3, 4, 5$.

$x_{j\mathrm{L}}$: lower bound of design variable.

$x_{j\mathrm{U}}$: upper bound of design variable.

F_{i0}: initial maximum load on main bearing over a period time, $i = 1, 2, 3, 4, 5, 6$.

In the design of crankshaft structure, system uncertainty is caused by various factors, such as structure parameters, system forecast model, sampling technology, judgments criterion. and human factors. Accordingly, reliability optimization is adopted to control and eliminate system uncertainty.

The reliability system-level optimization model can be represented as

$$\begin{aligned} \min \quad & M \\ \text{s.t.} \quad & J_i(Z) < \varepsilon \quad i = 1, 2, \ldots, n. \end{aligned} \tag{15}$$

The reliability subsystem-level optimization objective can be represented as

$$\begin{aligned} \min \quad & J_i(Z) = \left|X_i - Z_i\right|^2 \\ \text{s.t.} \quad & P\left[\sigma_{\max} < [\sigma]\right] - \Phi(\beta) \le 0 \\ & P\left[\theta_{\max} \le [\theta]\right] - \Phi(\beta) \le 0 \\ & P\left[F_i \le F_{i0}\right] - \Phi(\beta) \le 0 \quad i = 1, 2, \ldots, 6 \\ & X_{j\mathrm{L}} \le X_j \le X_{j\mathrm{U}} \quad j = 1, 2, \ldots, 5. \end{aligned} \tag{16}$$

The meaning of the symbols in the formula is shown as follows:

$P(\bullet)$: probability of failure constrains.

β: reliability index.

$\Phi(\beta)$: first-order estimate of reliability which obeys the normal distribution.

The determined optimization and reliability optimization are operated independently on the basis of MIGA. The advanced options of MIGA are listed in Table 2.

Table 2: Advanced options of MIGA.

Options	Parameter setting
Subpopulation size	20
Number of islands	10
Number of generations	50
Rate of crossover	0.8
Rate of mutation	0.0075
Rate of migration	0.25
Interval of migration	5
Relative tournament size	0.5
Elite	1.0

The initialization, range. and optimization results of each design variable are listed in Table 3.

The optimization results show that the weight of the crankshaft is reduced 7.2 kg, which accounts for 0.85% of the initial mass. However, the uncertain factors are not considered. The weight of the structure is reduced 5.9 kg through reliability optimization. The reliability optimization can not only achieve the lightweight of the crankshaft, but also ensure the reliability and robustness in engineering quality.

5.6. Multiobjective Optimization of MDO of Crankshaft Structure. According to formula (3), multiobjective optimization problem can be represented as

$$\begin{aligned} \min \quad & y = F(x) = \left(f_1(x), f_2(x), \ldots, f_n(x)\right) \\ \text{s.t.} \quad & x_{j\mathrm{L}} \le x \le x_{j\mathrm{U}} \quad j = 1, 2, \ldots, 5. \end{aligned} \tag{17}$$

Here, $f_i(x)$ $(i = 1, 2, \ldots, n)$ is the analysis target of designer, which can represent crankshaft mass, first-order modal frequency, second-order modal frequency, torsional angular vibration, the maximum stress over a period time, or the maximum main bearing load over a period time.

The range of the design variables and the optimization objectives need to be determined by actual production. MOP can be defined as tree-objective optimization when there are two optimization objectives in formula (17). Formula (17) can be represented as formula (18) where the torsional angular vibration and the maximum stress need to be optimized. Consider

$$\begin{aligned} \min \quad & y_2 = F_2(x) = w_1 f_1(x) + w_2 f_2(x) \\ \text{s.t.} \quad & x_{j\mathrm{L}} \le x \le x_{j\mathrm{U}} \quad j = 1, 2, \ldots, 5. \end{aligned} \tag{18}$$

Here, (w_1, w_2) is the weighting factor of $f_1(x)$ and $f_2(x)$.

Figures 16–18 show the biobject Pareto set of different weight values. Figure 19 shows the triobject Pareto set which regards the mass, the torsional angular vibration, and the maximum stress over a period time as the optimization goal.

In Figures 16–18, maximum stress increases with decreasing torsional angular vibration over a period time. Pareto set has changed with different weight values. Appropriate weight value needs to be determined by the requirement of the actual

Table 3: Design variables and optimization results.

Variables and response	Initialization	Upper bound	Lower bound	Deterministic optimal results	Reliability optimal results
x_1/mm	8.0	9.5	7.5	7.5	7.76
x_2/mm	16.0	18.0	14.0	17.9	16.9
x_3/mm	40.0	50.0	30.0	49.9	48.1
x_4/mm	40.0	50.0	30.0	49.9	46.3
x_5/mm	65.0	75.0	55.0	71.0	55.2
m/kg	846	—	—	838.8	840.1

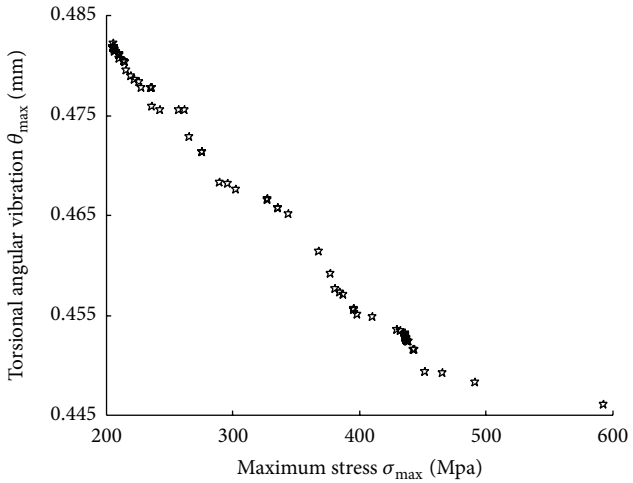

Figure 16: Pareto set with weight value (0.5, 0.5).

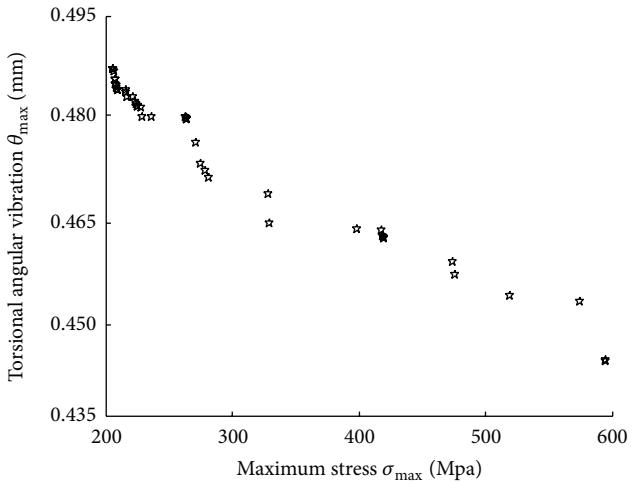

Figure 17: Pareto set with weight value (0.2, 0.8).

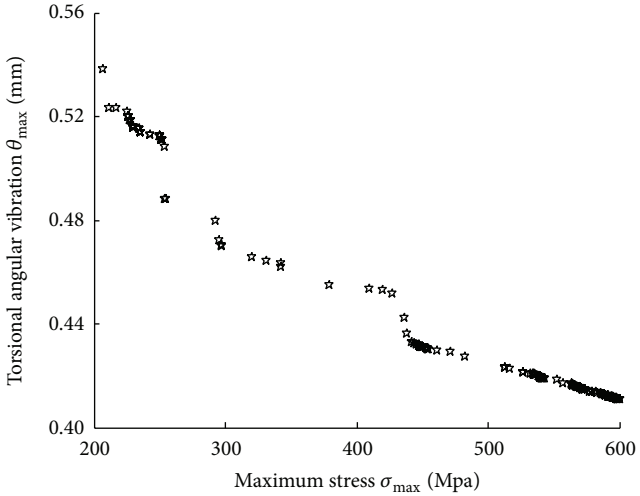

Figure 18: Pareto set with weight value (0.8, 0.2).

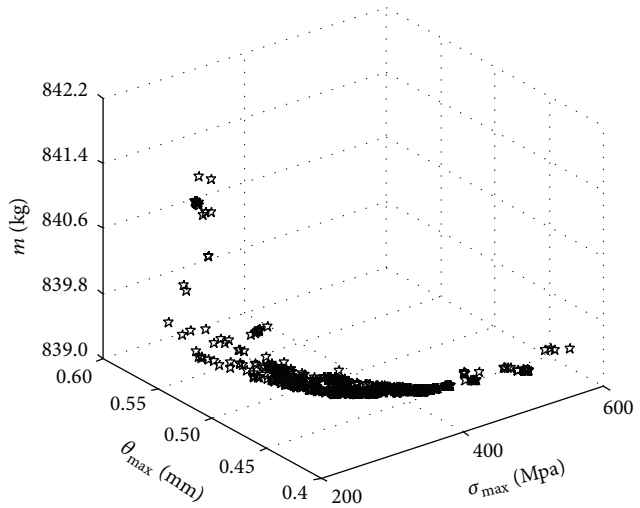

Figure 19: Pareto set with three optimization objects.

production. Then, the Pareto set is obtained and designers can choose the satisfactory optimization results.

In Figure 19, the weight value is set to (1, 1, 1). The values of mass, torsional angular vibration, and maximum stress over a period time are expected to achieve an optimal result. However, the paradoxical relationships are inevitably produced because of the coupled interactions. The improvement of one object is often at the expense of the decline of the other two. Appropriate weight value needs to be determined by the requirement of the actual production. Then, the Pareto set is obtained and designers can choose the satisfactory optimization results.

6. Conclusions

(1) The multidisciplinary optimization considering the crankshaft modal, torsional angular vibration, maximum stress over a period time and maximum load on the main bearings is operated on the basis of multi-island genetic algorithm, which can effectively improve the comprehensive property of the crankshaft.

(2) The parallel computing in multidisciplinary optimization is operated on the basis of the combination of elliptical basis function neural network theory and cooptimization method, which can enhance the optimization efficiency, so as to reduce product development cycle and costs.

(3) During the design optimization process of the crankshaft structure, the reliability design is combined with the cooptimization method. And the optimization of the crankshaft is operated on the basis of multi-island genetic algorithm, combined with design of experiment. The optimization can not only control the system uncertainty, but also ensure the reliability and robustness of the final optimal results of the crankshaft structure.

Competing Interests

The authors declares that there is no conflict of interests regarding the publication of this paper.

Acknowledgments

This work is supported by Open Fund (OGE201403-09) of Key Laboratory of Oil & Gas Equipment, Ministry of Education (Southwest Petroleum University), and ([2014]506) of Ministry of Industry and Information Technology (Manufacture of Marine High-Power Reciprocating Compressor).

References

[1] L. Murawski and A. Charchalis, "Simplified method of torsional vibration calculation of marine power transmission system," *Marine Structures*, vol. 39, pp. 335–349, 2014.

[2] Y. Yilmaz and G. Anlas, "An investigation of the effect of counterweight configuration on main bearing load and crankshaft bending stress," *Advances in Engineering Software*, vol. 40, no. 2, pp. 95–104, 2009.

[3] E. Larralde and R. Ocampo, "Selection of gas compressors: part 3," *World Pumps*, vol. 2012, no. 2, pp. 36–41, 2012.

[4] E. Larralde and R. Ocampo, "Selection of gas compressors: part 1," *World Pumps*, vol. 2011, no. 5, pp. 24–28, 2011.

[5] E. Larralde and R. Ocampo, "Selection of gas conpressors: part 2," *World Pumps*, no. 539, pp. 36–43, 2011.

[6] A. Almasi, "Reciprocating compressor optinmum design and manufacturing with respect to performance, reliability and cost," *Proceedings of World Academy of Science: Engineering & Technolog*, vol. 52, pp. 48–53, 2009.

[7] A. R. Health and P. M. McNamara, "Crankshaft stress analysis—combination of finite element and classical analysis techniques," *Journal of Engineering for Gas Turbines and Power*, vol. 112, no. 3, pp. 268–275, 1990.

[8] M. Rebbert, R. Lach, and P. Kley, "Dynamic crankshaft stress calculation using a combination of MSS and FEA," in *Proceedings of the International ADAMS User Meeting*, Orlando, Fla, USA, 2000.

[9] J. Raub, J. Jones, P. Kley, and M. Rebbert, "Analytical investigation of crankshaft dynamics as a virtual engine module," SAE Technical Paper 1999-01-1750, 1999.

[10] N. A. Warrior, A. P. Sime, T. H. Hyde, and H. Fessler, "The design of overlapped crankshafts Part 1: crankpin fillets," *Proceedings of the Institution of Mechanical Engineers, Part D: Journal of Automobile Engineering*, vol. 215, no. 4, pp. 503–513, 2001.

[11] B.-S. Yang, W.-W. Hwang, D.-J. Kim, and A. C. Tan, "Condition classification of small reciprocating compressor for refrigerators using artificial neural networks and support vector machines," *Mechanical Systems and Signal Processing*, vol. 19, no. 2, pp. 371–390, 2005.

[12] E. Benini, "Three-dimensional multi-objective design optimization of a transonic compressor rotor," *Journal of Propulsion and Power*, vol. 20, no. 3, pp. 559–565, 2004.

[13] S. Ho, Y.-L. Lee, H.-T. Kang, and C. J. Wang, "Optimization of a crankshaft rolling process for durability," *International Journal of Fatigue*, vol. 31, no. 5, pp. 799–808, 2009.

[14] S. Kodiyalam, R. J. Yang, L. Gu, and C.-H. Tho, "Multidisciplinary design optimization of a vehicle system in a scalable, high performance computing environment," *Structural and Multidisciplinary Optimization*, vol. 26, no. 3-4, pp. 256–263, 2004.

[15] A. Messac and A. Ismail-Yahaya, "Multiobjective robust design using physical programming," *Structural and Multidisciplinary Optimization*, vol. 23, no. 5, pp. 357–371, 2002.

[16] S. Koetniyom, P. C. Brooks, and D. C. Barton, "The development of a material model for cast iron that can be used for brake system analysis," *Proceedings of the Institution of Mechanical Engineers, Part D: Journal of Automobile Engineering*, vol. 216, no. 5, pp. 349–362, 2002.

[17] H. Lu, D. Yu, and Z. Xie, "Optimization of vehicle disc brakes stability based on response surface method," *Chinese Journal of Mechanical Engineering*, vol. 49, no. 9, pp. 55–60, 2013.

[18] S. Pierret, R. Filomeno Coelho, and H. Kato, "Multidisciplinary and multiple operating points shape optimization of three-dimensional compressor blades," *Structural and Multidisciplinary Optimization*, vol. 33, no. 1, pp. 61–70, 2007.

[19] S. Rabeau, P. Dépincé, and F. Bennis, "Collaborative optimization of complex systems: a multidisciplinary approach," *International Journal on Interactive Design and Manufacturing*, vol. 1, no. 4, pp. 209–218, 2007.

[20] K. Tamura, D. Peterson, N. Peterson, G. Stecher, M. Nei, and S. Kumar, "MEGA5: molecular evolutionary genetics analysis using maximum likelihood, evolutionary distance, and maximum parsimony methods," *Molecular Biology and Evolution*, vol. 28, no. 10, pp. 2731–2739, 2011.

[21] A. Ratnaweera, S. K. Halgamuge, and H. C. Watson, "Self-organizing hierarchical particle swarm optimizer with time-varying acceleration coefficients," *IEEE Transactions on Evolutionary Computation*, vol. 8, no. 3, pp. 240–255, 2004.

[22] M. Dorigo and C. Blum, "Ant colony optimization theory: a survey," *Theoretical Computer Science*, vol. 344, no. 2-3, pp. 243–278, 2005.

[23] M. Bühl and H. Kabrede, "Geometries of transition-metal complexes from density-functional theory," *Journal of Chemical Theory and Computation*, vol. 2, no. 5, pp. 1282–1290, 2006.

[24] J. M. Molero, E. M. Garzon, I. Garcia, and A. Plaza, "Analysis and optimizations of global and local versions of the RX algorithm for anomaly detection in hyperspectral data," *IEEE Journal of Selected Topics in Applied Earth Observations and Remote Sensing*, vol. 6, no. 2, pp. 801–814, 2013.

[25] H. Chen, R. Ooka, and S. Kato, "Study on optimum design method for pleasant outdoor thermal environment using genetic algorithms (GA) and coupled simulation of convection, radiation and conduction," *Building and Environment*, vol. 43, no. 1, pp. 18–30, 2008.